DTD 5

ARTICLE IN PRESS

Available online at www.sciencedirect.com

SCIENCE DIRECT®

Applied Surface Science xxx (2005) xxx–xxx

applied surface science

www.elsevier.com/locate/apsusc

Characterization of microroughness parameters in gadolinium oxide thin films: A study based on extended power spectral density analyses

M. Senthilkumar, N.K. Sahoo *, S. Thakur, R.B. Tokas

Spectroscopy Division, Bhabha Atomic Research Centre, Modular Laboratories, Trombay, Mumbai 400 085, India

Received 1 December 2004; received in revised form 28 February 2005; accepted 28 February 2005

Abstract

Spectral microroughness is a performance-limiting factor for optical thin films like Gd_2O_3, which have dedicative applications in ultraviolet or deep ultraviolet region of the electromagnetic spectrum. Such a morphological parameter of a thin film surface can be very well characterized by power spectral density (PSD) functions. The PSD provides a more reliable description to the topography than the RMS roughness and imparts several useful information of the surface including fractal and superstructure contributions. Through the present study it has been noticed that deposition parameters like evaporation rate and oxygen pressure can play very definite, dominant and predictable roles in the evolution of fractal and superstructures in thin film topographies recorded through atomic force microscopy (AFM). In this work, the PSD functions derived from morphologies of various gadolinia thin films have been fitted with a novel multi peak-shifting Gaussian model along with fractal and *k*-correlation functions, to extract characteristic parameters of the precision surfaces. Using such information, roughness contributions of the fractal components (substrate dominated), pure film and the aggregates have been successfully extracted. Higher spectral fractal strengths have depicted lower refractive index values. The microroughness and grain sizes of the pure film have been influenced very differently with deposition rate and oxygen pressure. The oxygen pressure strongly influenced the grain sizes where as the deposition rate influenced the microroughness of the gadolinia films.

PACS: 42.79W; 68.35.C; 61.16C; 81.15E

Keywords: Reactive electron beam evaporation; Surface microroughness; Power spectral density

1. Introduction

Because of the growth in the field of the semiconductor technology, the optical coating requirements in the ultraviolet (UV) and deep ultraviolet (DUV) region have been facing severe challenges to

* Corresponding author. Tel.: +91 22 25593871; fax: +91 22 25505151.
E-mail address: nksahoo@apsara.barc.ernet.in (N.K. Sahoo).

0169-4332/$ – see front matter © 2005 Elsevier B.V. All rights reserved.
doi:10.1016/j.apsusc.2005.02.122

meet the development criteria [1]. For example, deep UV photolithography with an ArF excimer laser source at a wavelength of 193 nm has been identified as a very attractive candidate for this potential process. The most preferable oxide optical coating materials are unsuitable in this spectral region due to their low band gap values. Although fluorides have some favourable transmission properties, because of their poor index ratios an excessive high number of layers are required to achieve the desired reflectivity in this wavelength region. Recently it has been demonstrated that electron beam deposited gadolinia (Gd_2O_3) films under low substrate temperatures can be very conveniently used to 193 nm (ArF) spectral region due to its favourable band gap values [2,3]. Most notably, the optical coating performance-limiting factors in this spectral region is predominantly decided by the quality of the microstructure and overall morphology of such thin films. For a reactively electron beam evaporated gadolinium oxide thin film at low substrate temperature, deposition rate and oxygen pressure can have strong influences on the grain structure as well as morphology evolutions. In order to design and develop an efficient low scattering multilayer device, it is essential to explore such parametric dependence of the surface topography.

In general, the microroughness characterization of a thin film surface can be carried out using optical or mechanical profiler or an atomic force microscope (AFM). However, AFM can be advantageously used with high vertical and spatial resolution to extract microroughness information of the surfaces [4]. Such roughness information obtained from AFM can be advantageously employed to the successful development of low scatter optical multilayer coatings. In addition, such information about the surface roughness is extremely useful for the alternate optical characterization of thin films using ellipsometry or spectrophotometry.

As mentioned above, gadolinia films deposited at lower substrate temperature exhibit high band gaps, which is very useful for developing deep UV optical coatings. Hence, in the present study, main thrust has been given to the films deposited under such substrate conditions. Several samples of gadolinium oxide films have been prepared using reactive electron beam evaporation technique by varying the deposition rate and oxygen pressure. The surface height profiles of the films have been measured using atomic force microscopy with different pre-decided scan sizes. The power spectral density (PSD) functions of all the surface profiles of each film have been computed and combined in to a single PSD profile covering large spatial frequency bandwidth. These experimentally derived PSDs have been fitted with appropriate analytical models. During our investigation, some of the experimental PSD profiles have exhibited more than one local maximum at lower spatial frequency region suggesting the presence of superstructures in the films. Hence, the existing PSD models have been suitably modified to account for the superstructures present in such thin films. From this fitting, the surface characteristic parameters relating to fractal properties (substrate dominated), roughness information of pure film and aggregates have been obtained for all the gadolinia films. Such information has helped to understand the influence of deposition conditions on microroughness introduced by the fractal components, pure film and the aggregates. In addition, one can advantageously use such information in tailoring a surface morphology according to the requirements by choosing appropriate deposition conditions.

In the present investigation concerning reactive electron beam deposition, the two process parameters such as deposition rate and oxygen pressure have been observed to affect the surface morphology very differently. The oxygen pressure depicted a stronger influence on surface lateral features (grain size) of pure films than the rate of evaporation. On the other hand, deposition rate has shown a stronger influence on RMS roughness of gadolinia films than the oxygen pressure. The deposition rate has also demonstrated a stronger influence on fractal nature of the films than the oxygen pressure. Besides, the higher values of fractal strengths have been observed to be associated with lower refractive indices. Aggregates have been invariably found in all the films deposited at low substrate temperature conditions. However, the microroughness of the film due to aggregates increases with the increase in oxygen pressure. The details of the surface topographic study are presented in the subsequent sections.

2. Microroughness characterization

As mentioned earlier, the microroughness or morphology of an optical surface is most popularly

characterized by the power spectral density (PSD) functions. PSD functions describe two aspects of the surface roughness such as the spread of heights from a mean plane, and the lateral distance over which the height variation occurs [5]. Hence, PSD explains a surface much better than the RMS roughness and provides very useful information on fractals and superstructures that may coexist in the microstructures. It has been realized recently that the fractal geometry and scaling concepts can concisely describe the rough surface morphology [6,7]. The surface morphology at different scales is believed to be self-similar and related in the fractal geometry. The ability of fractal analyses to extract many different types of information from measured textures compared to common, conventional analyses makes this approach very useful in describing surface characteristics of thin films. Several studies have demonstrated that the complexity of thin film morphology were fractal in nature, and can be characterized quantitatively by the fractal strengths and their dimensions as well [6,7]. Such an analysis employing the PSD information over a large spatial frequency scale has been applied to the present gadolinium oxide thin film surfaces. The following section puts some light on the PSD and its analysis techniques.

2.1. Thin films and power spectral density functions

The power spectral density function of thin films can be derived from the measurements of the bi-directional reflectance distribution function (BRDF) or from surface profiles measured by an optical or mechanical profiler or from the AFM surface profile data [5]. Amongst these techniques, AFM is an excellent tool for characterizing the surfaces and widely being used in studying optical thin film surfaces.

There have been large numbers of publications dealing with PSD calculations from the surface profile data. The computation of PSD function adopted in this paper is given by [8],

$$S_2(f_x, f_y) = \frac{1}{L^2}\left[\sum_{m=1}^{N}\sum_{n=1}^{N} Z_{mn}\, \mathrm{e}^{-e\pi \mathrm{i}\Delta L(f_x m + f_y n)} (\Delta L)^2\right]^2 \quad (1)$$

where S_2 denotes the two-dimensional PSD, L^2 is the scanned surface area, N is the number of data points per line and row, Z_{mn} is the profile height at position (m, n), f_x, f_y are the spatial frequency in the x- and y-directions and $\Delta L = N/L$ is the sampling distance.

This computation is further followed by the transition to polar co-ordinates in frequency space and angular averaging ($\{\varphi\}$)

$$S_2(f) = \frac{1}{2\pi}\int_0^{2\pi} S_2(f, \varphi)\, \mathrm{d}\varphi \quad (2)$$

As the PSD function depends on only one parameter, it is plotted in all our figures as a ''slice'' of the two dimensional representation. It remains a two dimensional function with a unit of fourth power to the length, i.e., ''$(\text{length})^4$''.

Conventionally, PSD functions obtained from AFM measurements have roughness values in a limited range of spatial frequencies. The range depends on the scan length and sampling distance, and it also can be additionally restricted or constrained by the effect of measurements artifacts. These limitations, however, can be overcome when the topographic measurements performed on different scales are appropriately combined, provided it fulfills following two conditions:

(i) The spatial frequency ranges where the measurements are defined should partially overlap. The condition is easy to meet by adequate selection of the scan sizes and the sampling distances.
(ii) In the overlapping region, the different PSD functions should be the same order of magnitude.

With these criteria, the combined PSD function at a desired frequency is described by the geometrical average and it is given by,

$$\mathrm{PSD}_{\mathrm{combined}}(f) = \left[\prod_{i=1}^{N} \mathrm{PSD}_i(f)\right]^{1/N} \quad (3)$$

where N is the number of PSD functions overlapping at the concern frequency. In the present work, the measurements have been performed at the same position and with three different scan sizes: 0.45 μm × 0.45 μm, 2 μm × 2 μm and 5 μm × 5 μm. The PSD functions have been computed separately for each scan. The values so obtained have been suitably

combined and averaged in order to obtain PSD for the desired extended spatial frequency range. To interpret an experimental PSD function an appropriate analytical model is highly essential which provide deep insight to the microscopic parametric dependence. Next section highlights this aspect of model based PSD interpretation.

2.2. PSD models for the microroughness interpretation

As described earlier, the PSD contains a more complete description than the RMS roughness and provides useful quantitative information of a thin film surface morphology. However, appropriate analytical models aid to the interpretation and understanding of such morphologies more qualitatively. In the past, several such models have been used to describe specific optical surfaces and thin films. These models consist of a function or combination of functions approximating the experimental PSD functional behavior. The most favourable extended model for the PSD of a thin film coating uses the sum of Henkel transforms of Gaussian and exponential autocorrelation function [9–11]. This model has been extensively used and led to satisfactory results in some specific cases. However, such an approach has a deficiency when wide-range of spatial frequencies is considered. In general, PSD of a thin film coating can be approximated to a sum of PSD of the substrate and the PSD of the pure film [12]. Moreover, in order to describe the surface roughness over large range of spatial frequencies, the PSD analytical model should include the mathematical term describing the overall roughness contribution from the substrate (fractals), pure film and aggregates. PSD of the substrates with spatial frequencies (f) mostly follows a fractal model, which obeys the inverse power law [13], i.e.,

$$\mathrm{PSD}_{\mathrm{fractal}}(f;K,\nu)=\frac{K}{f^{\nu+1}} \tag{4}$$

The intrinsic surface parameters describing such fractal-like surfaces are spectral strength (K) and spectral indices (ν) rather than RMS roughness (σ) and correlation length (l). This PSD form is obtained when it is assumed that the surface is self-affine, which is the case with varieties of precision substrates. The fractal dimension, "D" which some times mentioned by various experimentalists during the PSD analyses, is given by,

$$D=\tfrac{1}{2}(5-(\nu+1))=\tfrac{1}{2}(4-\nu),\quad \text{with } 0<\nu<2 \tag{5}$$

The dimension parameter has several meanings. For instance, the case $D=2$ ($\nu=0$) is called the extreme fractal; $D=1.5$ ($\nu=1$) the Brownian fractal; and $D=1$ ($\nu=2$) the marginal fractal.

Apart from substrate's fractal characteristics, sometimes, thin film coatings tend to develop fractal nature during the growth stages. The power spectra of most of our experimental PSD profiles of gadolinium oxide films exhibit similar characteristics especially at high spatial frequency regions, which indicate the presence of strong fractal components in the thin film topographies. It is, therefore, essential to include an appropriate fractal model to extract roughness contribution of fractal components from the total roughness of such thin films.

Morphological parameters and their analyses for the coated and uncoated substrates need different as well as appropriate insight to the characterization task. Fortunately, the function for describing the PSD of the pure film can be conveniently made use of the k-correlation model (also called as ABC model), which is given by [14,15],

$$\mathrm{PSD}_{\mathrm{ABC}}=\frac{A}{(1+B^2f^2)^{(C+1)/2}} \tag{6}$$

with A, B, C being parameters. This model satisfactorily describes random rough surfaces over large length scales. Eq. (6) gives a PSD function with a "knee," determined by B, which is equal to the correlation length. At small f values, well below the knee or the crossover region, the PSD is determined by A, and at high f values, beyond the knee, the surface is fractal and the PSD function is determined by C. However, the equivalent RMS roughness σ_{ABC} and correlation length τ_{ABC} that depend on these three parameters can be derived as follows:

$$\sigma^2_{\mathrm{ABC}}=\frac{2\pi A}{B^2(C-1)},\qquad \tau^2_{\mathrm{ABC}}=\frac{(C-1)^2B^2}{2\pi^2C} \tag{7}$$

All the above models are monotonically decreasing functions of spatial frequency and cannot account for any additional morphological features. However, it has been observed that several experimental thin films

show the formation of superstructures uniformly distributed along the surface. This induces a local maximum in the lower frequencies of the PSD that cannot be explained by any of such previous models. Modeling of such local maxima in PSDs can be carried out using a Gaussian function with its peak-maximum shifted to a non-zero spatial frequency as follows [16]:

$$\mathrm{PSD_{Sh}}(f;\sigma_{sh},\tau_{sh},f_{sh})=\pi\sigma_{sh}^2\tau_{sh}^2\exp[-\pi^2\tau_{sh}^2(f-f_{sh})^2] \quad (8)$$

This PSD corresponds to an autocovariance function with the form of a Gaussian multiplied by a cosine. The period of the cosine corresponds to the periodicity of the superstructures in the surface. The period is translated into the spatial frequency domain as the shift of the PSD maximum to the frequency f_{sh}. The meaning of the other model parameters can also be related to the various other characteristics of these superstructures. For example here, τ_{sh} corresponds to the size and σ_{sh} to the height of the superstructures.

In order to describe the PSD over a large spatial frequency bandwidth, Ferre-Borrull et al. [8], have used a model that includes above three Eqs. (4), (6) and (8). With this PSD model, they have satisfactorily characterized the surface topographies of ion beam sputtered MgF_2 thin film coatings. The PSD model used by them describes the experimental PSD behavior when there is only one local maximum in the profile. However, the most evaporated films like ours often exhibit superstructures having different values σ_{sh} and τ_{sh} distributed over the film surfaces. For such films, PSD exhibits more than one local maximum, which cannot be described using the above formalism. However, by adopting a combination of shifted Gaussian functions along with fractal and *k*-correlation functions it is possible to explain the presence of multiple local maxima. In the present investigation, such a multi peak-shifting Gaussian model approach has been employed, which is given by,

$$\mathrm{PSD_{total}}=\frac{K}{f^{\nu+1}}+\frac{A}{(1+B^2f^2)^{(C+1)/2}}+\sum_m \pi\sigma_{sh,m}^2\tau_{sh,m}^2\exp[-\pi^2\tau_{sh,m}^2(f-f_{sh,m})^2] \quad (9)$$

The experimental PSD curves of our gadolinia films have been fitted with this modified analytical model. As an example of this analysis method, experimental PSD of the films deposited at two different parametric conditions and their fitting results are presented in Fig. 1. The fractal roughness components of substrate, intrinsic film roughness and superstructures have been derived from this modeling. In Fig. 1(a) a local maximum at spatial frequency of 0.183 μm^{-1} is exhibited in the experimental PSD curve. However, in Fig. 1(b), two local maxima have been exhibited at 0.185 and 1.1 μm^{-1}. The goodness of the fit justifies the use of present analytical model for our evaporated films.

3. Experimental details

3.1. Sample preparation

Several thin film samples of Gd_2O_3 films have been deposited on quartz substrate using reactive electron beam evaporation techniques with the optical thickness of 8λ/4 (at λ = 600 nm). Optical thickness of the films has been monitored using Leybold's OMS-2000 optical monitor. The deposition rate of evaporation has been controlled using Inficon's XTC/2 quartz crystal monitor. During the deposition, the evaporation rate has been varied from 5 to 20 Å/s. However, the oxygen pressure has been varied from 0.5×10^{-4} to 2.0×10^{-4} mbar. Most of the films in the present study were deposited at the substrate temperature of 70 °C. This is because this film material, according to our earlier studies, has been observed to yield high optical band gap values (>6 eV) at such low and ambient substrate temperature deposition conditions. This happens to be a very useful as well as favourable property in making thin film optical multilayer devices for deep UV optical applications [2,3]. All the films have been subsequently characterized for surface topography using atomic force microscope.

3.2. Atomic force microscopy characterization

The surface topographic measurements have been carried out using NT-MDT's solver-P47H ambient based multimode atomic force microscope. The contact mode of AFM has been chosen for the topographic measurements. A silicon cantilever having typical radius of curvature of 10 nm, force

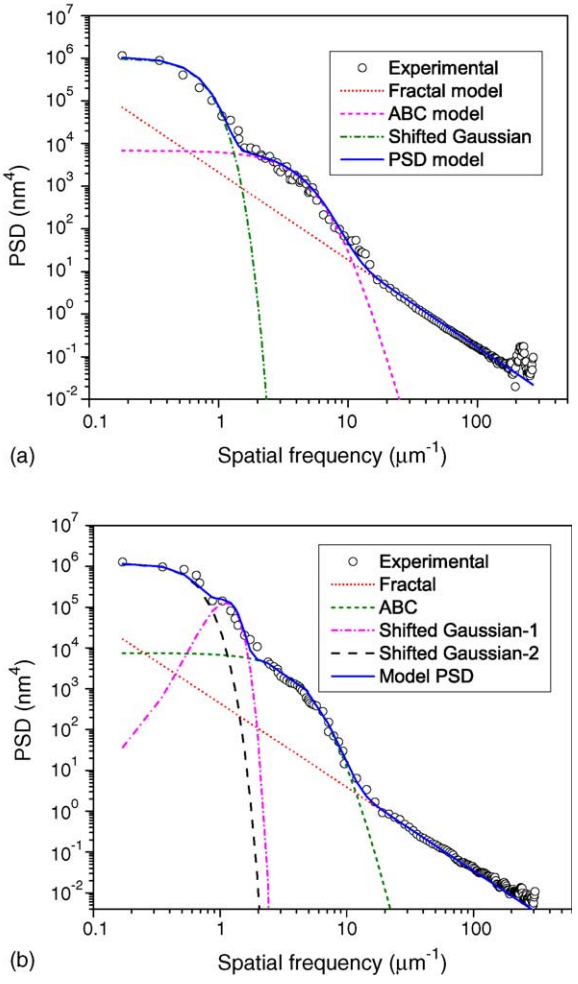

Fig. 1. Fitting of experimental PSD curves of gadolinium oxide films using an analytical model that consists of (a) one shifted Gaussian and (b) two shifted Gaussian, along with the fractal and ABC functions.

constant of 0.1 N/m and apex angle of 22° has been used for the measurements. Scans have been made over areas of 0.5 μm × 0.5 μm, 2 μm × 2 μm and 5 μm × 5 μm with the resolution of 256 pixels × 256 pixels for each film. Subsequently, the PSD functions have been calculated according to Eqs. (1) and (2) for all scan areas. By combining all the PSD functions according to Eq. (3), a PSD over a large spatial frequency bandwidth has been obtained. This procedure has been adopted for all the films deposited at different deposition conditions.

4. Results and discussions

The experimental PSD functions computed for the gadolinia films have been fitted with the analytical model described in Eq. (9). The least square minimization method has been employed to fit all the experimental PSD curves. The fitting parameters obtained from this procedure are presented in Table 1. In the present investigation, our prime objective is to study the surface topography of gadolinia films deposited at low ambient substrate temperature conditions. For a comparative study, a few films have also been deposited at elevated substrate temperature also. Such a comparison also highlights the importance and choice of lower substrate temperature values for the present gadolinia films.

4.1. Influence of the substrate temperature on microroughness

The topographies of the films deposited under elevated temperature conditions have shown distinct morphological changes. Such a measurement result has been compared here with the topographies of films deposited at low ambient conditions. Fig. 2 presents, the typical topographies of films deposited at the substrate temperatures of 70 and 250 °C respectively. During the deposition of these films, the oxygen pressure and deposition rate have been kept at 0.8×10^{-4} mbar and 10 Å/s respectively. In this figure, the topography of the film deposited at high substrate temperature depicts the presence of grain of similar sizes over the surface. In addition, they are distributed densely over the substrate. However, topography of the film deposited at low substrate temperature depicts the grains of different sizes, which are distributed over the surface. In addition, film deposited at elevated temperature has formed relatively larger grain sizes compared to the film deposited at lower substrate temperature. This observation can be attributed to the influence of surface mobility of the adatoms in the nucleation stages of the film growth. More qualitative information has been obtained from the PSD function of these surfaces and their characteristic parameters. The PSD functions computed for these films are presented in Fig. 3. It can be seen from this figure that the PSD function of the film deposited at the high substrate temperature shows

Table 1
Fitting coefficients of PSD spectra of Gd_2O_3 films deposited at different process conditions

Sample number	Deposition conditions			Fractal		k-correlation			Shifted Gaussian					
	Rate (Å/s)	O_2 pressure ($\times 10^{-4}$ mbar)	Substrate temperature (°C)	K (10^{-3} nm)	ν	A (10^2 nm)	B (nm)	C	Term-1			Term-2		
									σ_1 (nm)	τ_1 (nm)	x_1 (μm^{-1})	σ_2 (nm)	τ_2 (nm)	x_2 (μm^{-1})
1	5	0.8	70	1.9	1.0	14.5	125	4.6	0.6	320	0.65	–	–	–
2	10	0.8	70	1.3	1.02	92.0	95	7	0.5	150	0.3	0.23	510	0.4
3	15	0.8	70	6.0	1.00	160.0	230	5	0.4	10	2.055	–	–	–
4	20	0.8	70	8.13	1.05	265.0	225	7	0.39	400	0.35	–	–	–
5	10	0.5	70	0.31	1.05	75.5	130	12	0.21	980	1.1	0.7	800	0.185
6	10	0.8	70	1.3	1.02	92.0	95	7	0.5	150	0.3	0.23	510	0.4
7	10	1.5	70	1.5	1.05	65.5	130	10	0.78	690	0.183	–	–	–
8	10	2.0	70	0.5	1.15	105.0	230	5	0.72	450	0.42	–	–	–
9	10	0.8	250	6	1.0	99.3	330	2.2	0.496	300	0.3	–	–	–

Some of the films can be seen to fit very well with a single shifted-Gaussian term.

slower variation over the spatial frequency suggesting the larger lateral structures (grain size) present in this film than the PSD of the film deposited at low substrate temperature. In addition, mid and high spatial frequency regions depicts larger spectral roughness for the film deposited at elevated substrate temperature. The characteristic parameter extracted for these samples (sample nos. 2 and 9) are presented in Table 1. The intrinsic roughness parameters σ_{ABC} and τ_{ABC} calculated using Eq. (7) from the characteristic parameters for the film deposited at high substrate temperature are 0.69 and 54.85 nm respectively. Where as the values of σ_{ABC} and τ_{ABC} for the film deposited at low ambient substrate temperature are 0.33 and 45.49 nm respectively. It can be visualized from the PSD analysis that the film deposited at low substrate temperature yields lower intrinsic film roughness and lateral features compared to films deposited at high substrate temperatures.

In order to make complete understanding about the surface topographies of these films, it is necessary to analyze the remaining fractal components and aggregates (shifted Gaussian parameters) of the film. The PSDs of both the films exhibit inverse power law variation especially at the high spatial frequency region suggesting the presence of fractal components in the surface topographies. The spectral indices (ν) for the both the films are almost same (see Table 1). This is also evident from the high frequency regions of the PSD curve where the slopes of the PSD curve are same. However, the spectral strength (K) is higher in the case of the film deposited at high substrate temperature. This analysis concludes that the film deposited at higher substrate temperature appears to have stronger fractal components than the low temperature films.

It is well known that the low frequency components of the PSD spectrum represent the aggregates. The presence of such aggregates can be seen from the PSD spectra of these films. The low temperature films depicted higher spectral roughness at lower spatial frequency regions suggesting that aggregates have dominantly contributed to the roughness. This observation is a contrast to the film deposited at higher substrate temperatures. However, the intrinsic roughness of the film deposited at low substrate temperatures is low. Similar analyses have been carried out for such films deposited at different deposition rate and oxygen pressure. The details of the characterization of these films are presented in the following sections.

4.2. Influence of oxygen pressure

The oxygen pressure during the deposition not only controls the stoichiometry of the films but also influences the surface properties to a great extent. Fig. 4 depicts the PSD profiles of gadolinia films deposited at different oxygen pressure. It can be observed from this figure that the high spatial frequency regions for all films obey the inverse power law variation indicating a presence of strong fractal

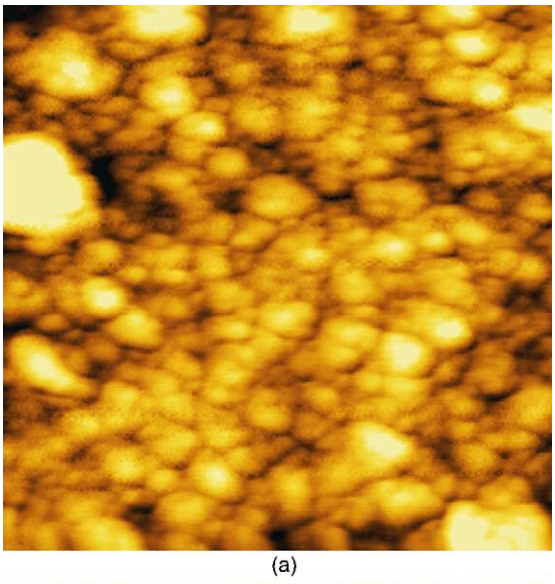

Fig. 2. Surface topography of gadolinium oxide films deposited at the substrate temperature of (a) 70 °C and (b) 250 °C. Scan area of these images is 1 μm × 1 μm.

components in the film topographies. The slopes of the PSDs in this region are almost same indicating all the films poses same values of fractal spectral indices (ν). However, the spectral strength (K) is noticed to vary in this region. In order to confirm this observation and to extract the intrinsic roughness of the films, the PSD profiles have been fitted with the model presented in

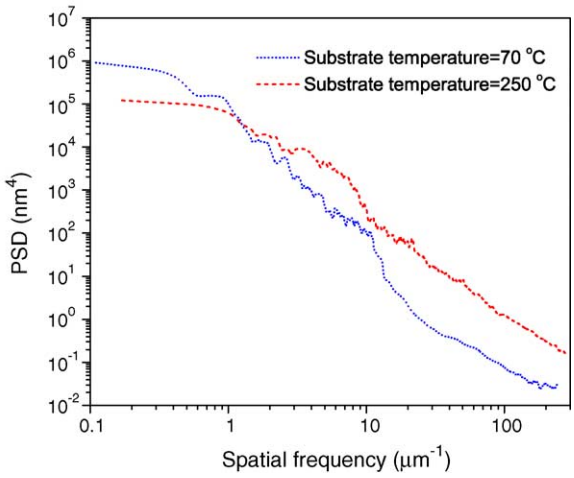

Fig. 3. The experimental PSD profiles of gadolinium oxide films deposited at 70 and 250 °C respectively.

Eq. (9). The characteristic parameters obtained from the fitting procedure are presented in Table 1. The plot of spectral strength computed for the films deposited at different oxygen pressure is shown in Fig. 5. It can be noted from this figure that the spectral strength is strongly influenced by the oxygen pressure. The lowest value of spectral strength has obtained for the film deposited at the oxygen pressure of 0.8×10^{-4} mbar. However, the spectral indices computed for these films have been varied from 1.02 to 1.15

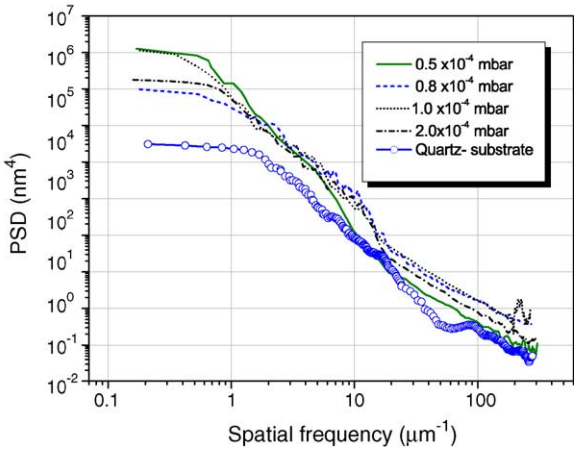

Fig. 4. The experimental PSD profiles of gadolinium oxide films deposited at different oxygen pressure. The deposition rate and substrate temperature during the deposition were fixed at 10 Å/s and 70 °C respectively.

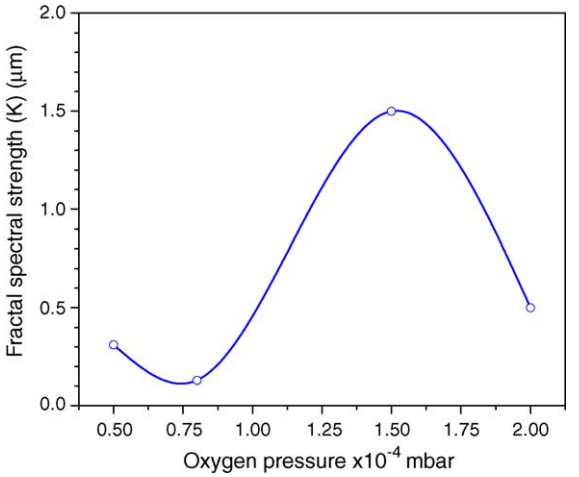

Fig. 5. The variation of fractal spectral strength (K) of the films deposited at different oxygen pressure. The deposition rate and substrate temperature during the deposition were fixed at 10 Å/s and 70 °C respectively.

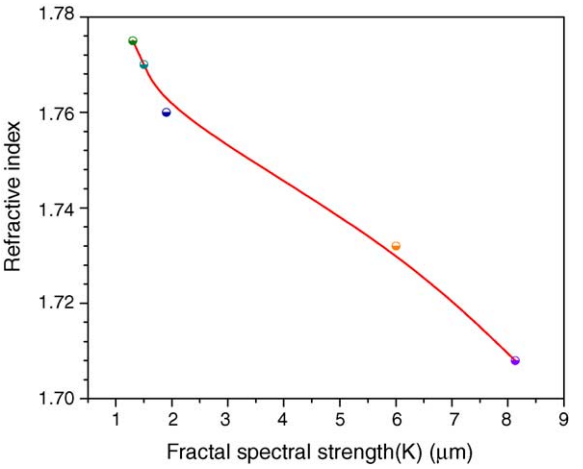

Fig. 6. The variation of refractive indices of the gadolinia films with fractal strength.

implying the dominance of Brownian fractals. One of the noteworthy observations is the correlation between the fractal strength and the refractive indices of the sample films. It can be seen from Fig. 6 that the lower values of the spectral fractal strengths are associated with the higher refractive indices and vice versa. Such an observation highlights a strong correlation between the morphology and the microstructure.

The roughness contribution of the pure film has been extracted using the k-correlation model. The RMS equivalent roughness (σ_{ABC}) and the correlation length (τ_{ABC}) have also been computed from the characteristic parameter obtained from the fitting procedure. The plots of σ_{ABC} and τ_{ABC} with oxygen pressure are presented in Fig. 7. As it can be seen from this figure that both the surface characteristic parameters have been influenced by the oxygen pressure. Besides, they follow a very similar functional trend. When, high oxygen pressure values have been adopted for the deposition, films have exhibited high values of RMS roughness and correlation length. However, at optimum oxygen pressure (0.8×10^{-4} mbar), films have demonstrated the lowest RMS roughness and correlation length. It can also be observed from this figure that the intrinsic roughness has varied from 0.33 to 0.56 nm. However, the correlation length has varied from 45.49 to 97.02 nm. It is, therefore, inferred that oxygen pressure alter the lateral features of these films more without causing appreciable changes in the RMS roughness.

4.3. Influence of the rate of deposition

The rate of evaporation has also influenced the surface properties of the gadolinia films to a great extent. Fig. 8 presents the PSD profiles of gadolinia films deposited at different rate of evaporation. Both the high and low spatial frequency regions of the PSD have been influenced by the deposition rate. However, the medium frequency region is not very much affected by this deposition parameter. It is observed from this figure that the high spatial frequency region of PSD for all films also obeys the inverse power law variation indicating the strong presence of fractal components. Besides, the slope of the PSD in this region is almost same indicating all the films pose same values for the fractal spectral indices (ν). However, the spectral strength (K) observed to vary in this spectral region. As mentioned earlier, the lower spatial frequency part of PSD function predominantly represents the aggregates. It is observed from this frequency region that aggregates contribute to the total film roughness to a large extent. In order to get the complete information about the surfaces, the PSD profiles were fitted with the model presented in Eq. (9). The characteristic parameter obtained from

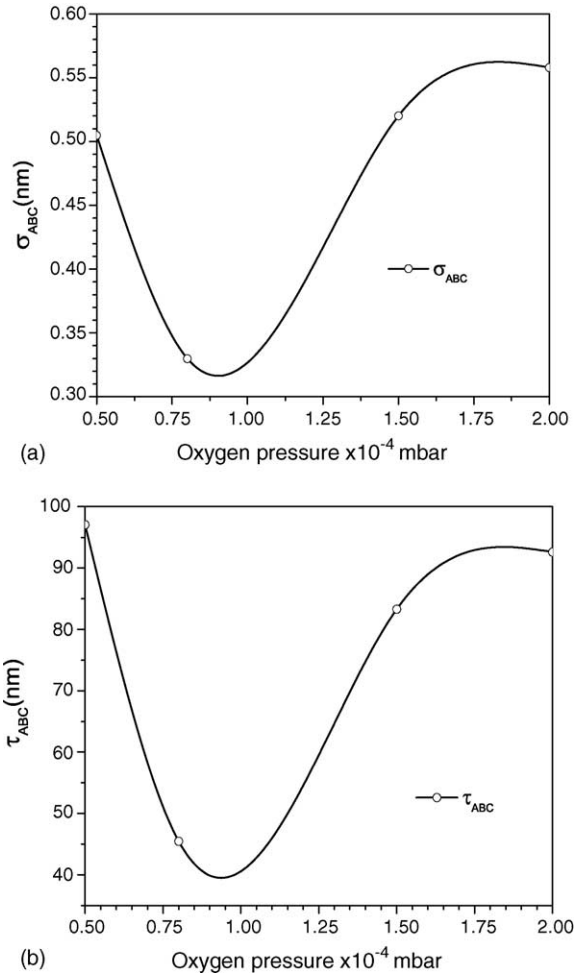

Fig. 7. Plots depicting the variation of (a) roughness (σ_{ABC}) and (b) correlation length (τ_{ABC}) with different oxygen pressure.

the fitting procedure is presented in Table 1. The plot of spectral strength computed for the films deposited at different deposition rate is shown in Fig. 9. The spectral strength (K) is varied from 1.3 to 8 μm with rate of evaporation. The lowest value of spectral strength is obtained for the film deposited at the deposition rate of 10 Å/s. However, the spectral indices computed for these films vary from 1.0 to 1.05. It is important to note that the spectral indices (ν) for the films deposited under different oxygen pressure and deposition rate are almost same. However, the spectral strength has been more influenced by the deposition rate than the oxygen pressure. It is therefore

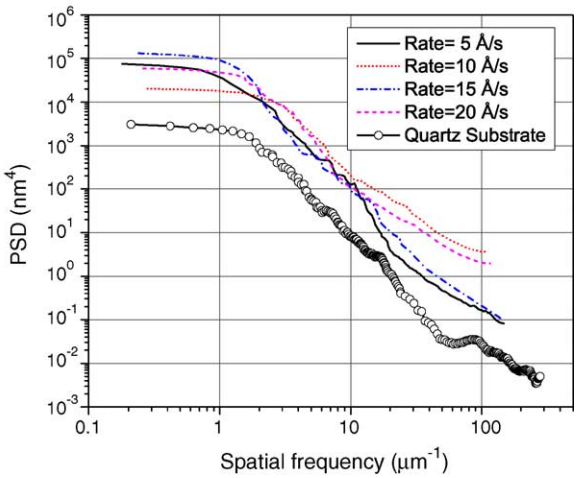

Fig. 8. The experimental PSD profiles of gadolinium oxide films deposited at different rate of evaporation. The oxygen pressure and substrate temperature during the deposition were fixed at 0.8×10^{-4} mbar and 70 °C respectively.

concluded that the deposition rate alters the fractal property more prominently than the oxygen pressure.

The roughness contribution of the pure film has also been extracted using the k-correlation model (ABC model). The RMS equivalent roughness (σ_{ABC}) and the correlation length(τ_{ABC}) have also been computed from the characteristic parameter obtained from Eq. (7). The plots of σ_{ABC} and τ_{ABC} with the rate

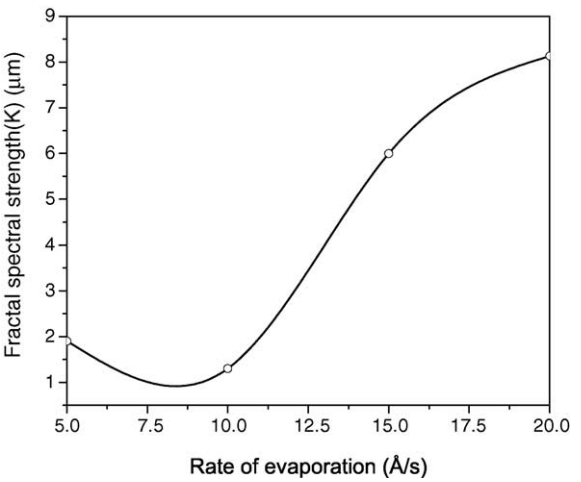

Fig. 9. The variation of fractal spectral strength (K) of the films deposited at different rate of evaporation. The oxygen pressure and substrate temperature during the deposition were fixed at 0.8×10^{-4} mbar and 70 °C respectively.

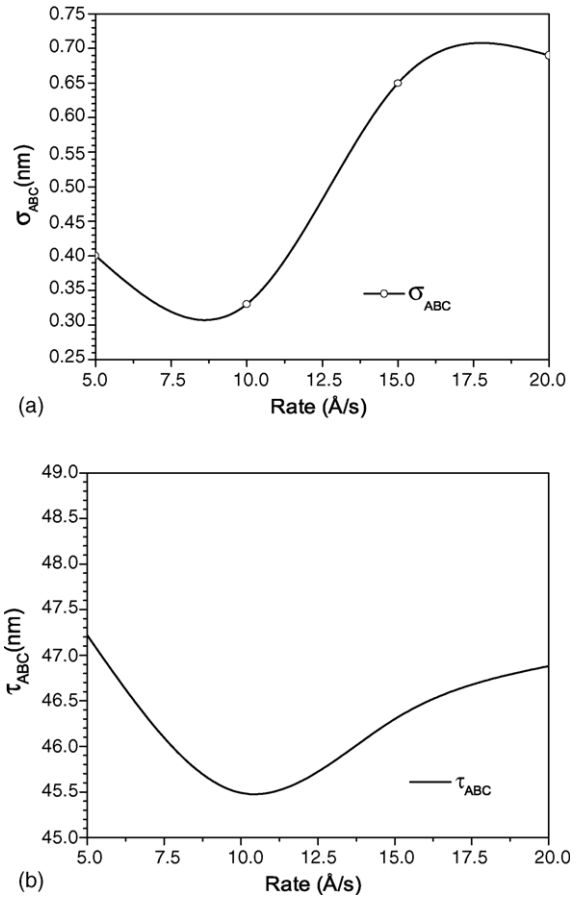

Fig. 10. Plots depicting the variation of (a) roughness (σ_{ABC}) and (b) correlation length (τ_{ABC}) with different rate of evaporation. The oxygen pressure and substrate temperature during the deposition were fixed at 0.8×10^{-4} mbar and 70 °C respectively.

of evaporation are presented in Fig. 10. Both the parameters shown in this figure have been influenced by the deposition rate. In addition, both the parameters follow the same trend with the deposition rate variation. With our present extreme rate of evaporation, the films have exhibited larger values in RMS roughness and correlation length. However, at optimum rate (10 Å/s), films yielded lowest RMS roughness and correlation length. It can also be observed from this figure that the intrinsic roughness has been varied from 0.33 to 0.69 nm. However, the correlation length has been varied from 45.49 to 47.22 nm. It is, therefore, inferred that deposition rate alters the vertical features (RMS roughness) of the film appreciably without causing much change in sizes of the lateral features of the films. This observation is in contrast to the influence of oxygen pressure on the film topography.

In the present investigation, both deposition rate and oxygen pressure have influenced the formation of aggregates. Variation of oxygen pressure has caused the formation of aggregates with sizes (τ_{sh}) ranging from 150 to 980 nm. Besides, their periodicity has been varied from 0.183 to 1.1 μm^{-1}. Where as the deposition rate variation has caused the formation of aggregates or superstructures with sizes (τ_{sh}) ranging from 10 to 500 nm. Their periodicity has been varied from 0.3 to 2.055 μm^{-1}. It can be easily visualized from this result that oxygen pressure has influenced the formation of relatively larger size aggregates (τ_{sh}) in the present thin film morphologies. In addition, such aggregates have been coarsely distributed over the surface. On the contrary, the deposition rate variation has influenced the formation of relatively smaller size aggregates that have been distributed densely over the film surface.

5. Conclusion

Reactive electron beam evaporated gadolinium oxide films have exhibited several interesting surface topographies. The effect of deposition rate and oxygen pressure on surface morphologies has been studied using detailed power spectral density analyses. The extended PSD profiles and the interpretation using the analytical models have yielded several interesting information about the fractals, intrinsic film roughness and aggregates of the thin film samples. The rate of evaporation depicted a strong influence on the microroughness of the pure film than the grain sizes. On the other hand, oxygen pressure has portrayed higher influence on the grain sizes than the microroughness of the pure film. Films deposited under various rates and oxygen pressure appeared to be mostly of Brownian fractal in nature. The spectral strength (K) of the fractal components of the surfaces has been influenced more by the rate of evaporation than the oxygen pressure. Both the parameters found to influence aggregates formation in the thin film during the growth process. In addition, fractal spectral strength has been strongly correlated with the refractive index of the film. In the present study, it

has been inferred that by systematically varying the process conditions, it is possible to achieve a relatively smooth morphology with an optimum parametric set. It is evident from our study that the optimum deposition condition (oxygen pressure = 0.8×10^{-4} mbar and deposition rate = 10 Å/s) yields this type of smooth and desirable morphology. Such process optimization is very essential to develop low scatter optical coatings for UV and deep UV laser applications.

References

[1] A. Duparre, Light scattering of thin dielectric films, Hand Book of Optical Properties, vol. 1, CRC Press, 1995.
[2] N.K. Sahoo, S. Thakur, M. Senthilkumar, D. Bhattacharyya, N.C. Das, Thin Solid Films 440 (2003) 155.
[3] N.K. Sahoo, M. Senthilkumar, S. Thakur, D. Bhattacharyya, N.C. Das, Appl. Surf. Sci. 200 (2002) 219.
[4] G. Binnig, C.F. Quate, C. Gerber, Phys. Rev. Lett. 56 (1986) 930.
[5] J.M. Elson, J.M. Bennett, Appl. Opt. 34 (1995) 201.
[6] A.J. Perry, Surf. Coat. Technol. 132 (2000) 21.
[7] W. Kwásny, L.A. Dobrzánski, M. Pawlyta, W. Gulbínski, J. Mater. Process. Technol. 157–158 (2004) 188–193.
[8] J. Ferre-Borrull, A. Duparre, E. Quesnel, Appl. Opt. 40 (2001) 2190.
[9] J.M. Elson, J.M. Bennett, J. Opt. Soc. Am. 69 (1979) 31.
[10] J.M. Elson, J.P. Rahn, J.M. Bennett, Appl. Opt. 19 (1980) 669.
[11] J.M. Elson, J.P. Rahn, J.M. Bennett, Appl. Opt. 22 (1983) 3207.
[12] S. Jakops, A. Duparre, H. Truckenbrodt, Appl. Opt. 37 (1998) 1180.
[13] E.L. Church, Appl. Opt. 22 (1988) 1518.
[14] E.L. Church, P.Z. Tackacs, T.A. Leonard, Proc. SPIE 1165 (1989) 136.
[15] G. Palasantzas, Phys. Rev. B 48 (1993) 14472.
[16] G. Rasigni, F. Varnier, M. Rasigni, J. Palmari, A. Llebaria, Phys. Rev. B 27 (1983) 819.